

# Spatial decoherence factor via the qubit-field interaction

A. Vaglica and G. Vetri

CNISM and Dipartimento di Scienze Fisiche ed Astronomiche, Università degli Studi di Palermo, via Archirafi 36, 90123 Palermo, Italy.

October 30, 2018

**Abstract.** We analyze the time evolution of an initial spatial coherence for a two level atom whose internal degrees of freedom interact with a single mode of a cavity field. When the qubit-field subsystem is taken as an environment, the translational dynamics experiences a decoherence process which may be encoded in a decoherence factor  $D$ . We find that the field statistics affects  $D$  through the alternative paths the system-environment may follow along their entanglement, while eventual field phase properties give rise to an imaginary part of  $D$  which is related to the atomic translation. From the decoherence perspective, we analyze the relation between the atomic momentum and the imaginary part of the atomic spatial density matrix, and some considerations on its asymptotic behavior are brought into question at the conclusion of the paper.

**PACS.** 03.65.Yz Decoherence; open systems; quantum statistical methods – 37.10.Vz Mechanical effects of light on atoms, molecules, and ions

## 1 Introduction

Decoherence program [1,2,3,4,5,6] may be considered a serious attempt to overcome the basic dilemma of Quantum Mechanics (QM): Why the world appears as classical, despite of its underlying quantum nature that allows for arbitrary superpositions of states? An implication inherent to this program is the possibility of dividing the world into subsystems. As suggested by Zeh [7,4], any obser-

vation involves ignorance of a subsystem (a part of the universe) and this procedure defines the "facts" that can be realized in a quantum system. Accordingly, Landsman [7,4] asserts that a measurement, a fact or event in QM implies the non-observation, or irrelevance, of a certain part of the system in question.

Remarkable experiments on the decoherence of mesoscopic coherent fields in a cat state and complementar-

ity experiments on Rydberg atoms interacting with microwave cavities have been performed by Brune et al. [8] (see also the review of Raimond, Brune, and Haroche [9]). Similar foundational aspects of complementarity, which-way information and quantum erasure have been studied by Storey, Collett, Walls [10,11], Scully, Englert, Walther [12], Storey, Tan, Collett, Walls [13], Dürr, Nonn, Rempe [14], in systems implying interactions and correlations among atomic internal and external dynamics and laser or maser cavities.

It is usually understood that the irrelevant subsystem works as a reservoir, that is, it consists of the innumerable degrees of freedom of the environment with which the system of interest interacts. However, in a natural way one may extend the analysis to environments with a few degrees of freedom (see for example [15,16,17]) and to pay attention to the role that the density of the states the irrelevant subsystem can effectively accede to, plays in the decoherence process. The study of these cases in which the system may follow a relatively small number of alternatives, can be useful for a grasp in the quantum-classical transition. For instance, non local correlations of entangled Bell's states may be suddenly and quite irreversibly destroyed by an environmental action of a subsystem of continuous one-degree of freedom [17]. Coherences and non local correlations are in fact very sensitive to any environmental action, and the ensuing information leakage towards the irrelevant part of the system is at the origin of the classical landing.

Decoherence effects on qubits caused by the atomic mo-

tion and, viceversa, effects of the qubit-field interaction on the atomic spatial coherences have been considered in different contexts (see for example [16,17,18,19,20,21,22,23,24]). In particular, in Ref. [23,24] the optical Stern-Gerlach (SG) model was used to analyze complementarity, which-path information and quantum erasure. Using the same model, the time behavior of the entanglement between the internal dynamics of a two-level atom, the zero point cavity field and the transverse translational variables of the atomic center of mass, was analytically studied in Ref. [20]. Disregarding the translational dynamics by tracing on the relative variables, the field-qubit coherences go to zero at long time. The diagonal form asymptotically attained by the reduced density matrix, clearly indicates how the field-qubit system goes towards the separability. In addition, if one choose the qubit as the system of interest, that is, tracing also on the field variables, one trivially recover the classical diagonal form of the qubit density matrix [25]. These are two examples of decoherence in which a decisive role is played by the irrelevance of a single degree of freedom, with a continuum of accessible states, that is, the conjugate variables that describe the atomic kinematics along the cavity axis.

In the present paper we will inquire on the atomic spatial coherences caused by the qubit-field interaction. Using the same model, we analyze the time evolution of an initial spacial coherence under the effect of the interaction between the field of an ideal cavity and the atomic internal dynamics. Looking at the qubit-field variables as the irrelevant part of our system, a decoherence

effect of the atomic position follows, and we show that the density matrix that describes the translational dynamics at a generic time  $t$  may be simply factorized in terms of the initial density matrix and a decoherence factor,  $\rho(x, x'; t) = \rho(x, x'; 0)D(x, x'; t)$ , where  $D(x, x'; t)$  will depend on the field statistics. We analyze the decoherence process for different initial configurations of the qubit-field subsystem. Starting from the more general state (pure or mixed) of the cavity single mode, we then specialize to some cases, including the thermal and coherent states. We also give the results for the so-called eigenstate of the Sussking-Glogower phase operator [26, 27, 28]. In all these cases we find a loss of coherences of the atomic position, similar to the well known phenomenon of the Rabi oscillations collapse in the usual Jaynes-Cummings model [29, 30, 31, 32, 33]. Because of the discreteness of the variables that account for our environment, a partial revival of the coherences follows at relatively long times.

Finally, we will address to the question of the decoherence process in the presence of a mean value of the atomic momentum. We find that for an increasing mean atomic momentum, as it is for some configurations here considered, the imaginary part of  $\rho(x, x'; t)$  does survive in some regions of the plane  $(x, x')$ .

## 2 Interaction of a travelling qubit with a single cavity mode

To pick up the spatial decoherence effect solely caused by the entanglement with the qubit-field subsystem, we will

consider Rydberg atoms interacting with microwave cavity field. The same kind of interaction is used by Scully et al. [12] in their analysis of complementarity, based on matter-wave interferometry. The possibility of realizing initial coherent spatial distributions using Rydberg atoms in microwave cavities, has actually been called in question in Ref. [11]. On the other hand, strong-coupling conditions readily obtained for these atoms and high quality factors  $Q$ , allow to neglect, with some accuracy, both spontaneous atomic emission ( $\tau_a \sim 10^{-2} \text{sec}$ ) and cavity loss ( $\tau_c \sim 10^{-3} \text{sec}$ ) [9] for the atomic flight times we will use to obtain full decoherence ( $T_0 \leq 10^{-3} \text{sec}$ ).

### 2.1 Model and initial configuration

The optical SG model is particularly suitable for an analytical study of our subject. It consists, as known, of the usual Jaynes-Cummings model in which, however, the dynamics of the atomic center of mass along the cavity axis is taken into account,

$$\hat{H} = \frac{\hat{p}^2}{2m} + \hbar\omega \left( \hat{a}^\dagger \hat{a} + \hat{S}_z + \frac{1}{2} \right) + \hbar\epsilon k \hat{x} (\hat{a}^\dagger \hat{S}_- + \hat{a} \hat{S}_+), \quad (1)$$

and correlates with the dynamics of the other subsystems. This Hamiltonian describes, in the rotating wave approximation, the resonant interaction of a two-level atom of mass  $m$  with the resonant  $k$ -mode of an ideal cavity. It is supposed that the atomic flight time inside the cavity is sufficiently small to treat classically the degree of freedom of the atomic center of mass along the direction orthogonal to the cavity axis. On the contrary, the atomic transverse dynamics in the  $x$ -direction, along the cavity axis, is quan-

tized and initially described by a packet of width narrow with respect to the wavelength  $\lambda$  of the resonant mode, and centered near a nodal region of the sinusoidal mode function. In these conditions it may be approximated by the linear term, as the interaction part of Eq. (1) shows. The conjugate variables  $\hat{x}$  and  $\hat{p}$  just describe this transverse dynamics,  $\hat{a}$  and  $\hat{a}^\dagger$  are the usual field operators, and  $\varepsilon$  is the atom-field coupling constant. Finally, the 1/2 spin operators  $\hat{S}_z$  and  $\hat{S}_\pm = \hat{S}_x \pm i\hat{S}_y$  account for the qubit dynamics.

The evolution operator for the Hamiltonian (1) may be factorized [28], for example, in the following form,

$$\begin{aligned} \hat{U}(t, 0) = & \exp \left\{ -\frac{2it}{\hbar} m \hat{a}_N \hat{\mu}_x \hat{x} \right\} \exp \left\{ -\frac{it}{2m\hbar} \hat{p}^2 \right\} \\ & \times \exp \left\{ \frac{i}{\hbar} \hat{a}_N t^2 \hat{\mu}_x \hat{p} \right\} e^{-i\vartheta_0(t)\hat{N}}, \quad t \leq T_0 \end{aligned} \quad (2)$$

where  $T_0$  indicates the atomic flight time inside the cavity, and

$$\hat{a}_N = a_0 \sqrt{\hat{N}}, \quad a_0 = \frac{\varepsilon \hbar k}{m}, \quad \vartheta_0(t) = \omega t + m a_0^2 t^3 / 6 \hbar \quad (3)$$

$$\hat{N} = (\hat{a}^\dagger \hat{a} + \hat{S}_z + \frac{1}{2}), \quad \hat{\mu}_x = \frac{\hat{a}^\dagger \hat{S}_- + \hat{a} \hat{S}_+}{2\sqrt{\hat{N}}}. \quad (4)$$

We suppose that the initial state of the entire system is given by

$$\hat{\rho}(0) = \hat{\rho}_t(0) \hat{\rho}_q(0) \hat{\rho}_f(0) \quad (5)$$

where

$$\hat{\rho}_t(0) = |\varphi(0)\rangle \langle \varphi(0)|, \quad \hat{\rho}_q(0) = |\varphi_q(0)\rangle \langle \varphi_q(0)| \quad (6)$$

account for the initial configuration of the atomic external and internal degrees of freedom, respectively, while

$$\hat{\rho}_f(0) = \sum_{n, n'} c_{n, n'} |n\rangle \langle n'| \quad (7)$$

describes a generic (pure or mixed) state of the cavity field, expressed in terms of Fock states  $|n\rangle$ . The qubit state

$|\varphi_q(0)\rangle$  is a coherent superposition

$$|\varphi_q(0)\rangle = \cos \frac{\gamma}{2} |e\rangle + e^{i\phi} \sin \frac{\gamma}{2} |g\rangle, \quad 0 \leq \gamma \leq \pi \quad (8)$$

of excited  $|e\rangle$  and ground  $|g\rangle$  states.

We are interested to the behavior of the atomic spatial coherences, so we consider a coherent superposition of two nearly distinct kets [2, 21],

$$|\varphi(0)\rangle = \frac{1}{\sqrt{2\delta}} [|\varphi_1(0)\rangle + |\varphi_2(0)\rangle] \quad (9)$$

to describe the initial position distribution of the atomic center of mass along the cavity axis. In particular, we will assume that the  $x$ -representation of  $|\varphi_j(0)\rangle$  ( $j = 1, 2$ ) is given by Gaussian functions,

$$\varphi_j(x, 0) = \left( \frac{1}{\sqrt{2\pi}\Delta x_0} \right)^{\frac{1}{2}} \exp \left\{ -\frac{(x - x_{0,j})^2}{4\Delta x_0^2} \right\}, \quad (10)$$

centered in  $x_{0,1}$  and  $x_{0,2}$ , respectively, around the origin of the reference frame which is set in a nodal point of the mode function. The normalization constant of state (9),

$$\delta = \left[ 1 + \exp \left\{ -\frac{(x_{0,1} - x_{0,2})^2}{8\Delta x_0^2} \right\} \right], \quad (11)$$

accounts for the eventual (small) overlap of the two Gaussians. For simplicity, the Gaussian distributions (10) are of minimum uncertainty,  $\Delta x_0 \Delta p_0 = \hbar/2$ , with the same widths  $\Delta x_0$  and  $\Delta p_0$  for both the Gaussians.

## 2.2 Time evolution of the full density operator

Let us consider the density operator  $\hat{\chi}(0) \equiv \hat{\rho}_q(0) \otimes \hat{\rho}_f(0)$  of the irrelevant subsystem. In terms of the dressed states

$$|\chi_n^\pm\rangle = \frac{1}{\sqrt{2}} [ |e, n\rangle \pm |g, n+1\rangle ], \quad |g, 0\rangle, \quad (12)$$

it assumes the following form

$$\begin{aligned} \hat{\chi}(0) = & \frac{1}{2} \sum_{n,n'=0}^{\infty} \{A_{n,n'} |\chi_n^+\rangle \langle \chi_{n'}^+| \\ & + B_{n,n'} |\chi_n^-\rangle \langle \chi_{n'}^-| + C_{n,n'} |\chi_n^+\rangle \langle \chi_{n'}^-\rangle\} \\ & + \frac{1}{2} \sum_{n=0}^{\infty} \{D_n (|\chi_n^+\rangle + |\chi_n^-\rangle) \langle g, 0| \\ & + E_n (|\chi_n^+\rangle - |\chi_n^-\rangle) \langle g, 0|\} + \frac{F}{2} |g, 0\rangle \langle g, 0| \\ & + h.c. \end{aligned} \quad (13)$$

where

$$\begin{aligned} A_{n,n'} = & \frac{1}{2} \{c_{n,n'} \cos^2(\gamma/2) + [c_{n,n'+1} e^{-i\phi} \\ & + c_{n+1,n'} e^{i\phi}] \cos(\gamma/2) \sin(\gamma/2) + c_{n+1,n'+1} \sin^2(\gamma/2)\} \end{aligned} \quad (14)$$

$$\begin{aligned} B_{n,n'} = & \frac{1}{2} \{c_{n,n'} \cos^2(\gamma/2) - [c_{n,n'+1} e^{-i\phi} \\ & + c_{n+1,n'} e^{i\phi}] \cos(\gamma/2) \sin(\gamma/2) + c_{n+1,n'+1} \sin^2(\gamma/2)\} \end{aligned} \quad (15)$$

$$\begin{aligned} C_{n,n'} = & \{c_{n,n'} \cos^2(\gamma/2) - [c_{n,n'+1} e^{-i\phi} - c_{n+1,n'} e^{i\phi}] \\ & \times \cos(\gamma/2) \sin(\gamma/2) - c_{n+1,n'+1} \sin^2(\gamma/2)\} \end{aligned} \quad (16)$$

$$D_n = \sqrt{2} \cos(\gamma/2) \sin(\gamma/2) c_{n,0} e^{-i\phi}, \quad (17)$$

$$E_n = \sqrt{2} \sin^2(\gamma/2) c_{n+1,0}, \quad (18)$$

$$F = \sin^2(\gamma/2) c_{0,0}. \quad (19)$$

We note that the dressed states (12) are eigenstates of the observables  $\hat{N}$  and  $\hat{\mu}_x$  which appear in the expression (2),

$$\hat{\mu}_x |\chi_n^\pm\rangle = \pm \frac{1}{2} |\chi_n^\pm\rangle, \quad \hat{N} |\chi_n^\pm\rangle = (n+1) |\chi_n^\pm\rangle. \quad (20)$$

Applying the evolution operator (2) to the initial state  $\hat{\rho}(0) = \hat{\rho}_t(0) \otimes \hat{\chi}(0)$  and using Eq.s (9), (13) and (20), we get the state of the entire system at time  $t \leq T_0$ ,

$$\begin{aligned} \hat{\rho}(t) = & \frac{1}{4\delta} \sum_{n,n'=0}^{\infty} e^{-i\vartheta_0(t)(n-n')} \{A_{n,n'} [|\phi_{n,1}^+(t)\rangle \\ & + |\phi_{n,2}^+(t)\rangle] [\langle \phi_{n',1}^+(t)| + \langle \phi_{n',2}^+(t)|] \otimes |\chi_n^+\rangle \langle \chi_{n'}^+| \\ & + B_{n,n'} [|\phi_{n,1}^-(t)\rangle + |\phi_{n,2}^-(t)\rangle] \end{aligned}$$

$$\begin{aligned} & \times [\langle \phi_{n',1}^-(t)| + \langle \phi_{n',2}^-(t)|] \otimes |\chi_n^-\rangle \langle \chi_{n'}^-| \\ & + C_{n,n'} [|\phi_{n,1}^+(t)\rangle + |\phi_{n,2}^+(t)\rangle] \\ & \times [\langle \phi_{n',1}^-(t)| + \langle \phi_{n',2}^-(t)|] \otimes |\chi_n^+\rangle \langle \chi_{n'}^-| \\ & + \frac{1}{4\delta} \sum_{n=0}^{\infty} e^{-i\vartheta_0(t)(n+1)} \{D_n [(\langle \phi_{n,1}^+(t)| + \langle \phi_{n,2}^+(t)|) |\chi_n^+\rangle \\ & + (\langle \phi_{n,1}^-(t)| + \langle \phi_{n,2}^-(t)|) |\chi_n^-\rangle] \langle g, 0| (\langle \varphi_1(t)| + \langle \varphi_2(t)|) \\ & + E_n [(\langle \phi_{n,1}^+(t)| + \langle \phi_{n,2}^+(t)|) |\chi_n^+\rangle - (\langle \phi_{n,1}^-(t)| \\ & + \langle \phi_{n,2}^-(t)|) |\chi_n^-\rangle] \langle g, 0| (\langle \varphi_1(t)| + \langle \varphi_2(t)|) \\ & + \frac{1}{4\delta} F |g, 0\rangle \langle g, 0| \otimes [|\varphi_1(t)\rangle + |\varphi_2(t)\rangle] [\langle \varphi_1(t)| + \langle \varphi_2(t)|] \\ & + h.c. \end{aligned} \quad (21)$$

where

$$|\varphi_j(t)\rangle = \exp\left\{-i \frac{\hat{p}^2 t}{2m\hbar}\right\} |\varphi_j(0)\rangle \quad (22)$$

describes the free evolution of the atomic center of mass for zero excitations in the qubit-field state, (last term of Eq. (13)), while

$$\begin{aligned} |\phi_{n,j}^\pm(t)\rangle = & \exp\left\{\mp \frac{i}{\hbar} m a_n t \hat{x}\right\} \exp\left\{-\frac{it}{2m\hbar} \hat{p}^2\right\} \\ & \times \exp\left\{\pm \frac{i}{2\hbar} a_n t^2 \hat{p}\right\} |\varphi_j(0)\rangle \end{aligned} \quad (23)$$

are the scattered components of the spatial atomic states due to the optical SG effect. In fact,  $a_n = a_0 \sqrt{n+1}$  accounts for the acceleration along the cavity axis of these components. In the  $x$ -representation one has

$$\begin{aligned} \phi_{n,j}^\pm(x,t) = & \left(\frac{\Delta x_0}{\sqrt{2\pi\beta(t)}}\right)^{\frac{1}{2}} \exp\left(\mp \frac{i}{\hbar} m a_n x t\right) \\ & \times \exp\left\{-\frac{[x - x_{n,j}^\pm(t)]^2}{4\beta(t)}\right\} \end{aligned} \quad (24)$$

with

$$x_{n,j}^\pm(t) = x_{0,j} \mp a_n t^2/2, \quad \beta(t) = \Delta x_0^2 + i\hbar t/2m. \quad (25)$$

For each value of  $n$  we get an uniformly accelerated Gaussian distribution, with the typical width of a free particle.

This behavior of the width is a consequence of the linearity of the positional potential energy which appears in the interaction term of the Hamiltonian (1).

### 3 Decoherence Factor

As said, in our case the irrelevant part is the qubit-field subsystem. In other words, we suppose to measure the atomic position whatever the values the qubit-field variables take on. From a mathematical point of view, this implies a tracing of the density operator  $\rho(t)$  on the field-qubit variables (for a discussion on the relation between a reduced density operator and the actual measurement of an observable, see [34,4]). In this section we give the exact expression of the reduced density matrix that describes the atomic translational dynamics. In addition, we will see that under sufficiently wide conditions, it is possible to single out a decoherence factor.

#### 3.1 Spatial density operator

Using the orthonormality of the dressed states (12) we get the following reduced density operator describing the atomic translation degree of freedom along the cavity axis,

$$\begin{aligned} \hat{\rho}_{space}(t) &= Tr_{field,qubit}[\hat{\rho}(t)] \\ &= \frac{1}{2\delta} \sum_{n=0}^{\infty} \{A_{n,n} [|\phi_{n,1}^+(t)\rangle + |\phi_{n,2}^+(t)\rangle] \\ &\quad \times [|\langle\phi_{n,1}^+(t)| + \langle\phi_{n,2}^+(t)|] + B_{n,n} \\ &\quad \times [|\phi_{n,1}^-(t)\rangle + |\phi_{n,2}^-(t)\rangle] [|\langle\phi_{n,1}^-(t)| + \langle\phi_{n,2}^-(t)|]\} \\ &\quad + \frac{1}{2\delta} F [|\varphi_1(t)\rangle + |\varphi_2(t)\rangle] [|\langle\varphi_1(t)| + \langle\varphi_2(t)|], \quad (26) \end{aligned}$$

where we have used the fact that the coefficients  $A_{n,n}$ ,  $B_{n,n}$  and  $F$  are real. To analyze the atomic spatial coherences, we take the matrix elements of  $\hat{\rho}_{space}(t)$  with respect to the position eigenstates. Using Eq.s (22) and (24), and separating the real and the imaginary parts of the exponents we get

$$\begin{aligned} \hat{\rho}(x, x'; t) &\equiv \langle x | \hat{\rho}_{space}(t) | x' \rangle \\ &= \frac{F}{2\delta\sqrt{2\pi}\Delta x_l(t)} \sum_{j,k=1}^2 \exp \left[ i\alpha_0^{j,k}(x, x') \right] \\ &\quad \times \exp \left\{ -\frac{1}{4\Delta x_l^2(t)} \left[ (x - x_{0,j})^2 + (x' - x_{0,k})^2 \right] \right\} \\ &\quad + \frac{1}{2\delta\sqrt{2\pi}\Delta x_l(t)} \sum_{n=0}^{\infty} \sum_{j,k=1}^2 A_{n,n} \exp \left[ i\alpha_{n,+}^{j,k}(x, x') \right] \\ &\quad \times \exp \left\{ -\frac{1}{4\Delta x_l^2(t)} \left[ (x - x_{n,+}^j(t))^2 + (x' - x_{n,+}^k(t))^2 \right] \right\} \\ &\quad + \frac{1}{2\delta\sqrt{2\pi}\Delta x_l(t)} \sum_{n=0}^{\infty} \sum_{j,k=1}^2 B_{n,n} \exp \left[ i\alpha_{n,-}^{j,k}(x, x') \right] \\ &\quad \times \exp \left\{ -\frac{1}{4\Delta x_l^2(t)} \left[ (x - x_{n,-}^j(t))^2 + (x' - x_{n,-}^k(t))^2 \right] \right\} \quad (27) \end{aligned}$$

where we have set

$$\begin{aligned} \alpha_0^{j,k}(x, x') &= \frac{\hbar t}{8m\Delta x_0^2\Delta x_l^2(t)} \\ &\quad \times \left[ (x - x_{0,j})^2 - (x' - x_{0,k})^2 \right] \quad (28) \end{aligned}$$

$$\begin{aligned} \alpha_{n,\pm}^{j,k}(x, x') &= \frac{\hbar t}{8m\Delta x_0^2\Delta x_l^2(t)} \left\{ [x - x_{n,j}^{\pm}(t)]^2 \right. \\ &\quad \left. - [x' - x_{n,k}^{\pm}(t)]^2 \right\} \mp \frac{1}{\hbar} m a_n t (x - x') \quad (29) \end{aligned}$$

and we have used

$$\Delta x_0^2 \Delta p_0^2 = \hbar^2 / 4 \quad (30)$$

$$|\beta(t)|^2 = \Delta x_0^2 (\Delta x_0^2 + \Delta p_0^2 t^2 / m^2) \equiv \Delta x_0^2 \Delta x_l^2(t). \quad (31)$$

Once again, we wish to stress that the Eq. (27) is the exact reduced density operator describing the atomic dynamics along the cavity axis in the optical SG model, for generic

states of the cavity field and the qubit. In the next section the decoherence process hidden in Eq. (27) will be analyzed for some specific states of the cavity field.

### 3.2 Decoherence factor

We now observe that the linear approximation of the cavity mode function requires small displacement and spread of the atomic wave packet, small with respect to the wavelength  $\lambda$ . In other words, when the atom leaves the cavity its spatial distribution must be essentially unchanged with respect to the initial one. As a consequence, the flight time  $T_0$  must be sufficiently short to allow the disregard of both the displacement  $a_n T_0^2/2$  and the distortion  $\Delta p_0 T_0/m$  in Eq.s (25) and (31). For the values of the parameters used in this paper, these conditions are fulfilled for  $T_0 \Omega \leq 10^3$ , where  $\Omega = \varepsilon \sqrt{\langle n \rangle + 1}$  is the Rabi frequency. For flight time satisfying this condition we have (see Eq.s (25) and (31))  $x_{n,j}^\pm(t) \simeq x_{0,j}$  and  $\Delta x_l^2(t) \simeq \Delta x_0^2$ . Consequently, Eq.s (28) and (29) become

$$\alpha_0^{j,k}(x, x') \simeq \frac{\hbar t}{8m\Delta x_0^4} \left[ (x - x_{0,j})^2 - (x' - x_{0,k})^2 \right] \quad (32)$$

$$\alpha_{n,\pm}^{j,k}(x, x') \simeq \alpha_0^{j,k}(x, x') \mp \frac{1}{\hbar} m a_n t (x - x'). \quad (33)$$

As for  $\alpha_0^{j,k}(x, x')$ , the values of the parameters used in the paper give  $\max \left\{ \alpha_0^{j,k}(x, x') \right\} \leq 10^{-3}$ , and the phase factors in the second and third terms of Eq. (27) will only depend on  $m a_n t (x - x')/\hbar$  which takes into account the optical SG effects in the atomic momentum distribution.

Taking into account all these approximations, the Eq. (27) may be written as the product of the initial spatial density matrix and a decoherence factor,

$$\hat{\rho}(x, x'; t) \simeq \hat{\rho}(x, x'; 0) D(x, x'; t) \quad (34)$$

where

$$\hat{\rho}(x, x'; 0) = \frac{1}{2\delta\sqrt{2\pi}\Delta x_0} \times \sum_{j,k=1}^2 \exp \left\{ -\frac{1}{4\Delta x_0^2} \left[ (x - x_{0,j})^2 + (x' - x_{0,k})^2 \right] \right\}, \quad (35)$$

$$D(x, x'; t) = \sum_{n=0}^{\infty} \{ (A_{n,n} + B_{n,n}) \cos [k(x - x') \Omega_n t] - i(A_{n,n} - B_{n,n}) \sin [k(x - x') \Omega_n t] \} + F, \quad (36)$$

and

$$\Omega_n = \Omega \sqrt{\frac{n+1}{\langle n \rangle + 1}}, \quad \Omega = \varepsilon \sqrt{\langle n \rangle + 1}. \quad (37)$$

Expression (34) is of easy reading and, at the same time, a very good approximation. In fact, all the figures describing the decoherence effects presented below, has been obtained from this equation, but actually they cannot be distinguished from those related to the exact expression (27).

Expression (36) is suitable also to explicate the relation between the field coherence properties and the one-sided atomic deflection [28] in the optical SG effect. A mean value of  $\hat{p}$  different from zero requires an imaginary part of the density operator. For an initial real density operator as in our case this implies, for  $t > 0$ ,  $Im[D(x, x'; t)] \neq 0$ , that is  $A_{nn} \neq B_{nn}$ . In fact, it is not difficult to show that

$$\langle \hat{p} \rangle (t) = \hbar k \sum_{n=0}^{\infty} (B_{n,n} - A_{n,n}) \Omega_n t. \quad (38)$$

Looking at Eq.s (14) and (15), we conclude that the atomic center of mass may acquire an increasing momentum along the cavity axis if its qubit interacts with a field that owns

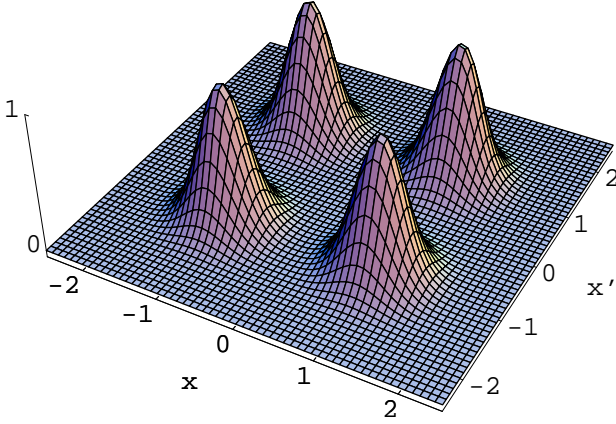


**Fig. 1.** This figure shows the reduced density matrix  $\hat{\rho}(x, x'; 0)$  of Eq. (35) and represents the initial condition for all the cases considered below. It describes the initial atomic populations (near the  $x = x'$  direction) and coherences (near the  $x = -x'$  direction) for the position degree of freedom along the cavity axis. The values of the parameters are:  $m = 10^{-25}$  kg,  $\varepsilon = 10^5 \text{ sec}^{-1}$ ,  $\lambda = 0.6 \times 10^{-2}$  meters,  $\Delta x_0 = \lambda/100$ ,  $x_{0,1} = -\lambda/20$ ,  $x_{0,2} = \lambda/20$ . The positions  $x, x'$  are considered in units of  $|x_{0,1}|$ . coherence properties, that is, when  $c_{n,n'}$  is not proportional to  $\delta_{n,n'}$ .

## 4 Some examples of field statistics

In this section the behavior of the atomic spatial coherences will be studied considering some examples of field states. To this end, it is sufficient to specialize the coefficients  $A_{n,n}, B_{n,n}$  and  $F$  of Eq.s (14-19), according to the specific initial field state, and then use Eq. (36). The spatial initial condition for all the cases here considered is given by  $\hat{\rho}(x, x'; 0)$  of Eq. (35), and shown in Fig. 1. Under appropriate conditions [2], the two peaks near the  $x = x'$

direction evolve towards the atomic populations (the two possible atomic positions) for the translational degree of freedom along the cavity axis, while the peaks near the orthogonal direction,  $x = -x'$ , undergo a quenching when the system evolves towards a classical behavior.

### 4.1 Incoherent field states

From our particular point of view, a common interesting feature of the incoherent field states is the equality, for each  $n$ , of the coefficients  $A_{n,n}$  and  $B_{n,n}$  in Eq. (36), that implies the reality of  $D(x, x'; t)$  and, in our case, of  $\hat{\rho}(x, x'; t)$ .

#### 4.1.1 Thermal state

A cavity field in a thermal state at the temperature  $T$  is described by the normalized Boltzmann factor,

$$\begin{aligned} \hat{\rho}_f(0) &= \frac{e^{-\beta_B \hbar \omega \hat{a}^\dagger \hat{a}}}{\text{Tr}(e^{-\beta_B \hbar \omega \hat{a}^\dagger \hat{a}})} \\ &= (1 - e^{-\beta_B \hbar \omega}) \sum_{n=0}^{\infty} e^{-n\beta_B \hbar \omega} |n\rangle \langle n| \end{aligned} \quad (39)$$

where  $\beta_B = 1/k_B T$  and  $k_B$  is the Boltzmann constant.

Comparison with Eq. (7) gives

$$c_{n,n'} = (1 - e^{-\beta_B \hbar \omega}) e^{-n\beta_B \hbar \omega} \delta_{n,n'}. \quad (40)$$

Consequently, for the coefficients  $A_{n,n}, B_{n,n}$  and  $F$  of Eq.s (14), (15) and (19) we have

$$\begin{aligned} A_{n,n} = B_{n,n} &= \frac{1}{2} (1 - e^{-\beta_B \hbar \omega}) e^{-n\beta_B \hbar \omega} \\ &\times \{ \cos^2(\gamma/2) + e^{-\beta_B \hbar \omega} \sin^2(\gamma/2) \} \end{aligned} \quad (41)$$

$$F = \sin^2(\gamma/2) (1 - e^{-\beta_B \hbar \omega}). \quad (42)$$



As said, the equality  $A_{n,n} = B_{n,n}$  implies that the decoherence factor,

$$\begin{aligned}
D(x, x'; t) &= \sin^2(\gamma/2) (1 - e^{-\beta_B \hbar \omega}) \\
&+ (1 - e^{-\beta_B \hbar \omega}) [\cos^2(\gamma/2) + e^{-\beta_B \hbar \omega} \sin^2(\gamma/2)] \\
&\times \sum_{n=0}^{\infty} \cos[k(x - x') \Omega_n t] e^{-n\beta_B \hbar \omega}. \quad (43)
\end{aligned}$$

is a real function. The corresponding density matrix  $\hat{\rho}(x, x'; t) = \hat{\rho}(x, x'; 0) D(x, x'; t)$  is shown in Fig. 2. The entanglement with the field-qubit environment causes a spatial coherence decay (upper), followed by a very partial revival (lower), because of the discreteness of the states to which the environment can accede. It is evident that by increasing  $T$  the revivals should be postponed in time.

One may also analyze the coherence behavior by looking at the function  $\hat{\rho}(x, x'; t)$  along the  $x' = -x$  direction. Fig. 3 shows a temporal sequence of the function  $\hat{\rho}(x' = -x; t)$  for the same thermal case. In what follows, the spatial coherences will be only analyzed in terms of function of this kind.

#### 4.1.2 Coherent state with random phase

A mixture of coherent states with random phases is given by

$$\begin{aligned}
\hat{\rho}_f(0) &= \frac{1}{2\pi} \int_0^{2\pi} d\vartheta |\alpha\rangle \langle \alpha| \\
&= e^{-|\alpha|^2} \sum_{n=0}^{\infty} \frac{\alpha^{2n}}{n!} |n\rangle \langle n|. \quad (44)
\end{aligned}$$

In this case we have

$$c_{n,n'} = \frac{\alpha^{2n}}{n!} e^{-|\alpha|^2} \delta_{n,n'} \quad (45)$$

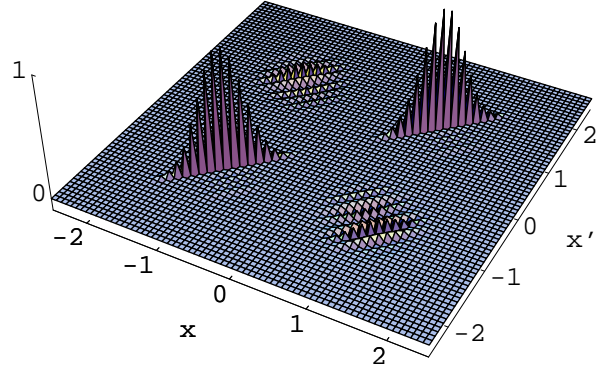
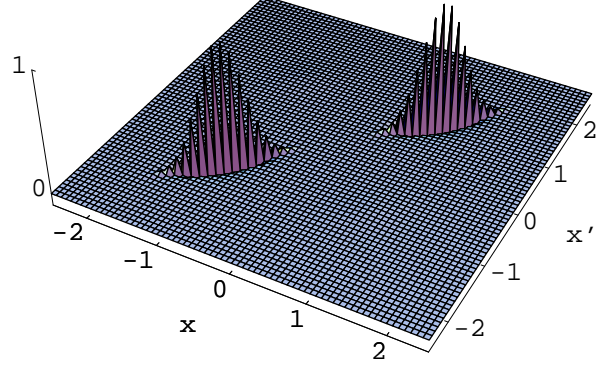


**Fig. 2.** Position density operator  $\hat{\rho}(x, x'; t)$  of Eq. (34) at time  $t = 100 \Omega^{-1}$  (upper) and  $t = 1000 \Omega^{-1}$  (lower), when the field is in the thermal state (39), and the decoherence factor  $D(x, x'; t)$  is given by Eq. (43). The parameter values of the cavity and the qubit are:  $T = 200^\circ K$ , corresponding to  $\langle n \rangle \simeq 82.76$  and  $\gamma = \pi/2$ . The other parameters are as in Fig.1.

and using Eq.s (14-19) we obtain

$$A_{n,n} = B_{n,n} = \frac{|\alpha|^{2n}}{2n!} e^{-|\alpha|^2} \left[ \cos^2 \frac{\gamma}{2} + \frac{|\alpha|^2}{n+1} \sin^2 \frac{\gamma}{2} \right] \quad (46)$$

$$F = e^{-|\alpha|^2} \sin^2(\gamma/2). \quad (47)$$

The decoherence function,

$$D(x, x'; t) = e^{-|\alpha|^2} \sin^2(\gamma/2) + e^{-|\alpha|^2} \sum_{n=0}^{\infty} \frac{|\alpha|^{2n}}{n!} \times \left( \cos^2 \frac{\gamma}{2} + \frac{|\alpha|^2}{n+1} \sin^2 \frac{\gamma}{2} \right) \cos [k(x-x') \Omega_n t] \quad (48)$$

is equal to real part of the same function relative to the coherent state (see sec. 4.2.1). Consequently, Fig. 5 describes also this case.

### 4.1.3 Fock state

Finally, for a Fock state

$$\hat{\rho}_f(0) = |n_0\rangle \langle n_0|, \quad (49)$$

it is  $c_{n,n'} = \delta_{n,n_0} \delta_{n',n_0}$ . Consequently, one has

$$A_{n,n} = B_{n,n} = \frac{1}{2} \left[ \delta_{n,n_0} \cos^2 \frac{\gamma}{2} + \delta_{n,n_0-1} \sin^2 \frac{\gamma}{2} \right], \quad (50)$$

$$F = \delta_{n_0,0} \sin^2(\gamma/2) \quad (51)$$

and

$$D(x, x'; t) = \cos^2(\gamma/2) \cos [k(x-x') \Omega_{n_0} t] + \sin^2(\gamma/2) \cos [k(x-x') \Omega_{n_0-1} t] + \sin^2(\gamma/2) \delta_{n_0,0}. \quad (52)$$

The behavior of  $\hat{\rho}(x' = -x; t)$  for the number case, shown in Fig. 4, outlines how the coherences survive at all times if the exchange of energy (and information) between the system of interest and the environment follows a few paths.

## 4.2 Field states with phase properties

When the field density matrix  $c_{n,n'} = \langle n | \hat{\rho}_f(0) | n' \rangle$  of Eq. (7) is not diagonal, the coefficients  $A_{n,n}$  and  $B_{n,n}$  of Eq. (36) may be different between them.  $D(x, x'; t)$  and  $\hat{\rho}(x, x'; t)$  are in general complex functions.

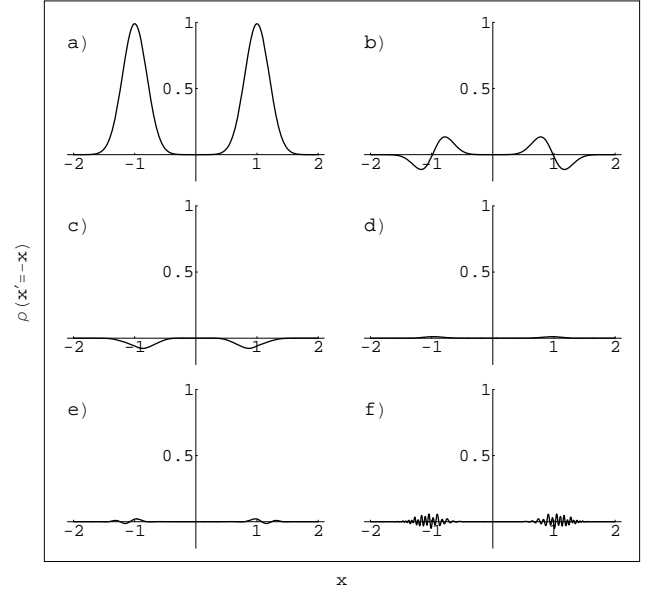


**Fig. 3.** This figure describes in a simple way the decoherence effect (followed by a partial revival, curve (f)), for the thermal state (39). It represents the function  $\hat{\rho}(x, x'; t)$  defined by Eqs (34), (35) and (43), along the  $x' = -x$  direction. From (a) to (f) time is 0, 3, 10, 100, 200, 500, in units of  $\Omega^{-1}$ . The other parameters are as in Fig. 2

### 4.2.1 Coherent state

For an initial coherent state of the cavity field,

$$\hat{\rho}_f(0) = e^{-|\alpha|^2} \sum_{n,n'=0}^{\infty} \frac{\alpha^n (\alpha^*)^{n'}}{\sqrt{n!n'}} |n\rangle \langle n'|, \quad (53)$$

we have

$$c_{n,n'} = \frac{\alpha^n (\alpha^*)^{n'}}{\sqrt{n!n'}} e^{-|\alpha|^2}; \quad \alpha = |\alpha| e^{i\theta} \quad (54)$$

and

$$A_{n,n} = \frac{|\alpha|^{2n}}{2n!} e^{-|\alpha|^2} \left| \cos \frac{\gamma}{2} + \frac{|\alpha| e^{i(\theta+\phi)}}{\sqrt{n+1}} \sin \frac{\gamma}{2} \right|^2 \quad (55)$$

$$B_{n,n} = \frac{|\alpha|^{2n}}{2n!} e^{-|\alpha|^2} \left| \cos \frac{\gamma}{2} - \frac{|\alpha| e^{i(\theta+\phi)}}{\sqrt{n+1}} \sin \frac{\gamma}{2} \right|^2, \quad (56)$$

while coefficient  $F$  is still given by Eq. (47). The decoherence factor is

$$D(x, x'; t) = e^{-|\alpha|^2} \sin^2(\gamma/2) + e^{-|\alpha|^2} \sum_{n=0}^{\infty} \frac{|\alpha|^{2n}}{n!}$$

$$\begin{aligned}
& \times \left( \cos^2 \frac{\gamma}{2} + \frac{|\alpha|^2}{n+1} \sin^2 \frac{\gamma}{2} \right) \cos [k(x-x') \Omega_n t] \\
& - 2i|\alpha|e^{-|\alpha|^2} \sin \gamma \cos(\theta + \phi) \\
& \times \sum_{n=0}^{\infty} \frac{|\alpha|^{2n}}{n! \sqrt{n+1}} \sin [k(x-x') \Omega_n t]. \quad (57)
\end{aligned}$$

whose real part coincides with the decoherence function (48). We recall that, for  $\langle n \rangle$  sufficiently large (as it is in our case) and  $\gamma = \pi/2$ , the phase relation between the qubit and the field may lead to two opposite behaviors. For  $\theta + \phi = \pi/2$  one has  $A_{n,n} \simeq B_{n,n}$ ,  $D(x, x'; t)$  and  $\hat{\rho}(x, x'; t)$  are real, and  $\langle \hat{p} \rangle (t) = 0$ . On the contrary, for  $\theta + \phi = 0$ , or  $\pi$  the decoherence factor is complex and a one-sided deflection characterizes the optical SG effect. In fact one has  $B_{n,n} = 0$ , or  $A_{n,n} = 0$ , respectively and the atom is scattered to left or to the right (see Eq. (38)). This is the so called trapping condition, after the fact that the qubit population is approximately trapped to the initial value, with the consequent quenching of the Rabi oscillations [35,28]. (For the relation between the interference phenomenon of the Rabi oscillations and the selective deflection in the optical SG model see Ref. [20]). For the case  $\theta + \phi = 0$  and  $\gamma = \pi/2$ , the behavior of the real and imaginary part of  $\hat{\rho}(x' = -x; t)$  is shown in Figs 5 and 6, respectively.

#### 4.2.2 Phase state

The exact coherent trapping condition [27,28] may be achieved when the cavity field is in an eigenstate of the Susskind-Glogower phase operator [26,27]  $\exp(i\hat{\theta}) = (\hat{n} +$

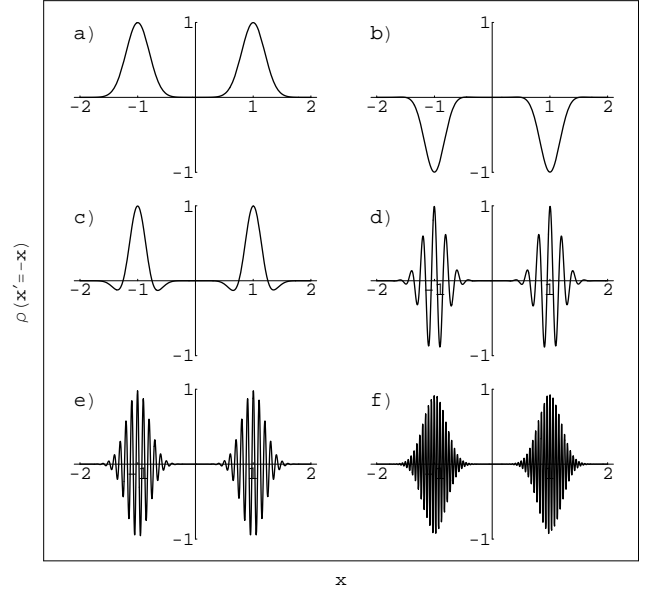


**Fig. 4.** Same quantity of Fig. 3 when the cavity field is in the Fock state (49), with  $n_0 = 83$ , and  $\gamma = \pi/2$ . From (a) to (f) time is 0, 5, 10, 50, 100, 200, in units of  $\Omega^{-1}$ . The other parameters are as in Fig. 1.

$1)^{-1/2}\hat{a}$ . In this case the field is

$$\hat{\rho}_f(0) = (1 - |z|^2) \sum_{n,n'=0}^{\infty} z^n (z^*)^{n'} |n\rangle \langle n'|. \quad (58)$$

and

$$c_{n,n'} = (1 - |z|^2) z^n (z^*)^{n'}. \quad (59)$$

The coherent trapping takes on for particular relations between the field and the qubit parameters. In fact, it is required that

$$z = e^{i\theta} \cot(\gamma/2), \quad \pi/2 < \gamma \leq \pi, \quad (60)$$

and  $\theta + \phi = 0$  or  $\pi$ .

By using Eq.s (14-19) and (59) we obtain

$$\begin{aligned}
A_{n,n} &= \frac{1}{2} (1 - |z|^2) |z|^{2n} \{ \cos^2(\gamma/2) \\
& + 2|z| \cos(\theta + \phi) \cos(\gamma/2) \sin(\gamma/2) + |z|^2 \sin^2(\gamma/2) \} \quad (61) \\
B_{n,n} &= \frac{1}{2} (1 - |z|^2) |z|^{2n} \{ \cos^2(\gamma/2)
\end{aligned}$$

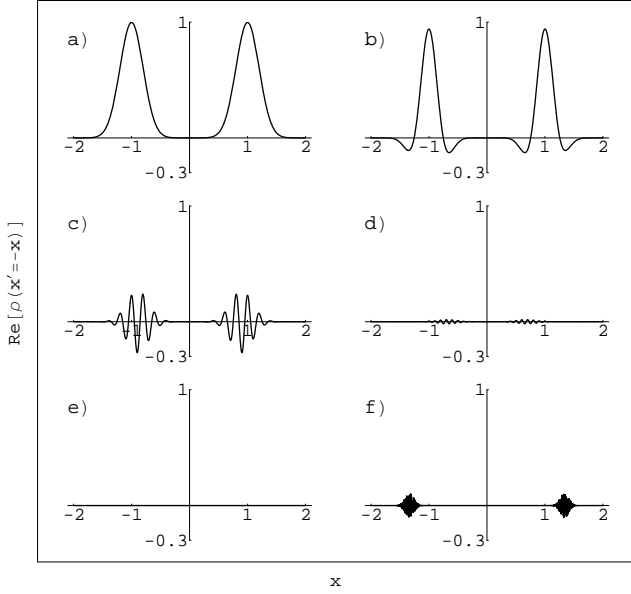


**Fig. 5.** Real part of  $\hat{\rho}(x' = -x; t)$  when the cavity field is in the coherent state (53) with  $|\alpha|^2 = \langle n \rangle = 82.76$ , and the field-qubit system is in the trapping configuration,  $\theta + \phi = 0$  and  $\gamma = \pi/2$ . From (a) to (f) time is 0, 10, 50, 100, 500, 1200, in units of  $\Omega^{-1}$ . The other parameters are as in Fig. 1. This figure describes also the behavior of  $\hat{\rho}(x' = -x; t)$  for the coherent state with random phase, see Eq.s (48) and (57).

$$-2|z| \cos(\theta + \phi) \cos(\gamma/2) \sin(\gamma/2) + |z|^2 \sin^2(\gamma/2) \} \quad (62)$$

$$F = \sin^2(\gamma/2)(1 - |z|^2) \quad (63)$$

As one can easily see, for  $\theta + \phi = 0$  ( $\theta + \phi = \pi$ ) one has  $B_{n,n} = 0$  ( $A_{n,n} = 0$ ). The previous consideration on the interplay between coherent trapping, quenching of the Rabi oscillations and selective atomic deflection in this case hold exactly. It is also to note that the photon distribution of state (58) follows a geometric law,

$$P_n = \langle n | \hat{\rho}_f(0) | n \rangle = (1 - |z|^2) |z|^{2n} = \frac{\langle n \rangle^n}{(1 + \langle n \rangle)^{n+1}} \quad (64)$$

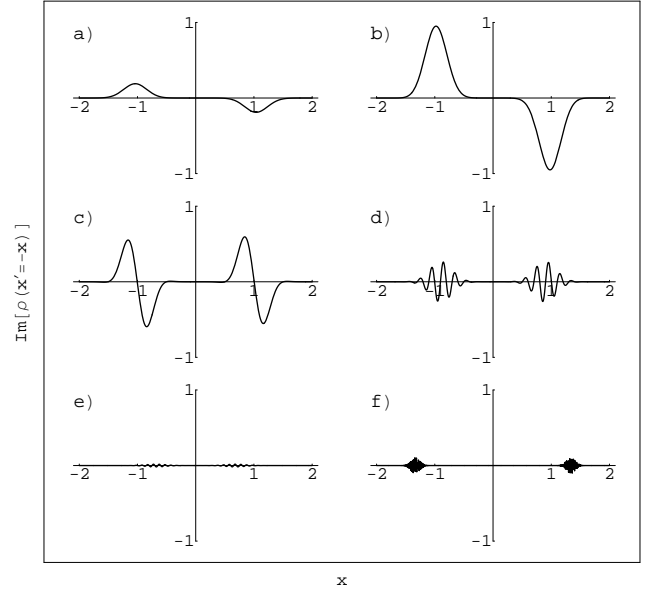


**Fig. 6.** Imaginary part of  $\hat{\rho}(x' = -x; t)$  for the same configuration of Fig. 5. This figure shows the growing (from zero) of the imaginary part of the atomic position coherence, followed by a loss and a partial revival. From (a) to (f) time, in units of  $\Omega^{-1}$ , is 0.3, 3, 10, 50, 100, 1200. The other parameters are as in Fig. 5

with

$$\langle n \rangle = \frac{|z|^2}{(1 - |z|^2)} = \frac{\cot^2(\gamma/2)}{(1 - \cot^2(\gamma/2))}. \quad (65)$$

The pure state (58) owns the same photon statistics of the mixed thermal state (39). For this reason, the behavior of  $Re[\hat{\rho}(x' = -x; t)]$  is very similar to the thermal case and, for the phase state, we report in Fig. 7 only  $Im[\hat{\rho}(x' = -x; t)]$ .

Comparing the standard deviations of the geometric distribution,  $\Delta n \simeq \langle n \rangle$  for large  $n$ , and of the Poissonian law,  $\Delta n = \sqrt{\langle n \rangle}$ , we may conclude that for the same value of  $\langle n \rangle$  the interaction with a thermal (or phase) state takes place following more alternatives with respect to the coherent case. As a consequence, coherences fall off

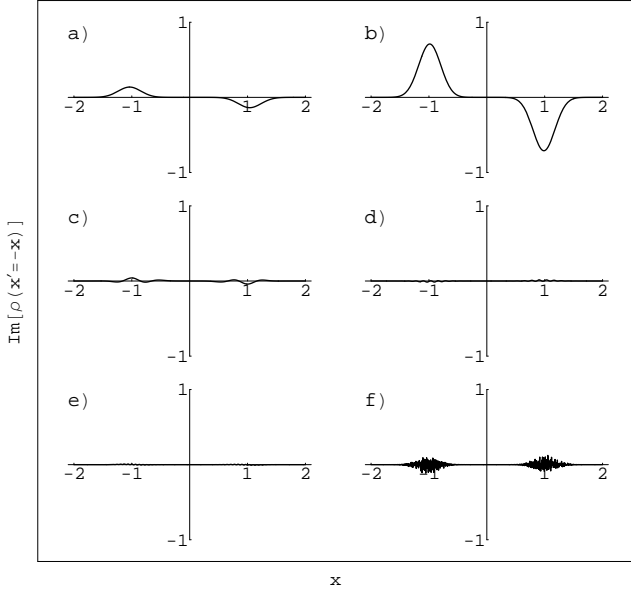


**Fig. 7.** Imaginary part of  $\hat{\rho}(x' = -x; t)$  for the phase state (58) in the trapping configuration ( $\theta + \phi = 0$ ), with  $\gamma = 0.5019115\pi$ , for which it is  $\langle n \rangle = 82.76$ . The other parameters are as in Fig. 6

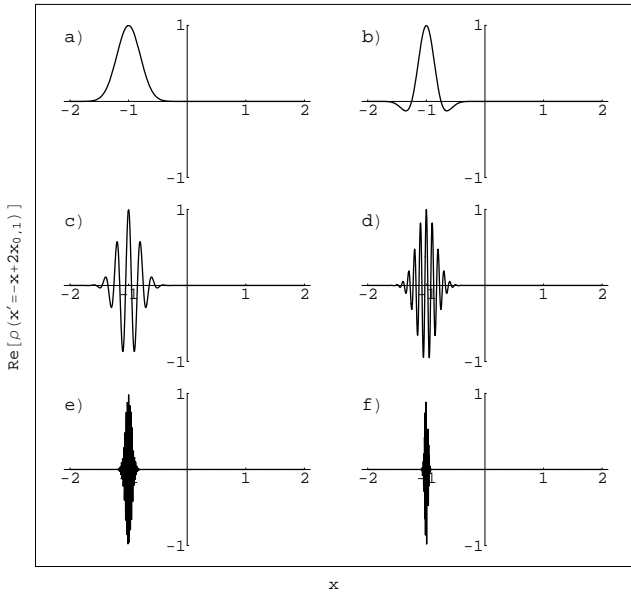


**Fig. 8.** Real part of  $\hat{\rho}(x' = -x + 2x_{0,1}; t)$  for the coherent state with  $|\alpha|^2 = 82.76$ , in the trapping configuration, ( $\theta + \phi = 0$ ) and  $\gamma = \pi/2$ . We recall that the position variable  $x$  is considered in units of  $|x_{0,1}|$ . From (a) to (f) time is 0, 10, 50, 100, 500, 1000, in units of  $\Omega^{-1}$ . The other parameters are as in Fig. 1

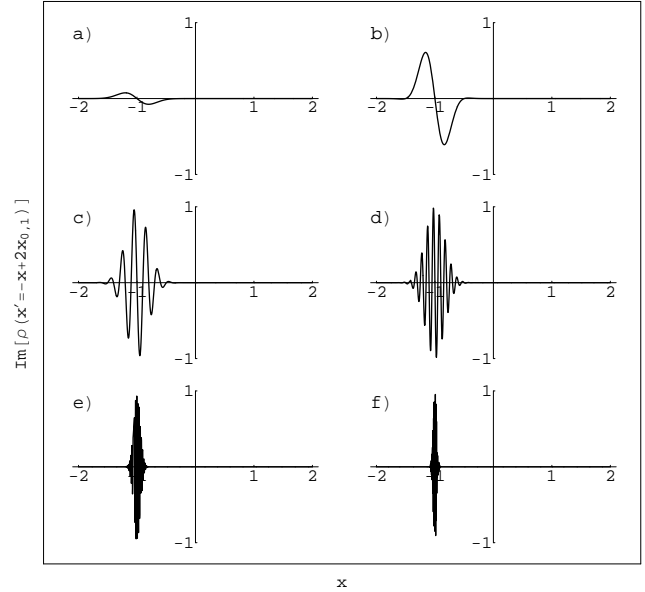


**Fig. 9.** Imaginary part of  $\hat{\rho}(x' = -x + 2x_{0,1}; t)$  for the coherent state of Fig. 6. From (a) to (f) time is 1, 10, 50, 100, 500, 1000, in units of  $\Omega^{-1}$ . The other parameters are as in Fig. 8

more quickly in the first case, as one can see comparing Figs 3 and 5 for the real part of the density matrix, and Figs 7 and 6 for the imaginary part.

It is to notice that the coherence revivals of Figs 5, 6 and 7 are displayed for times which are borderline with respect to the validity of the model.

## 5 Decoherence effects on local coherences

Let us come back briefly to the link between the imaginary part of the spatial density matrix and the atomic momentum. It may be interesting to note that this link involves some constraints to the decoherence process of the imaginary part of  $\hat{\rho}(x, x'; t)$ , at least in some regions of the plane  $(x, x')$ . Consider again Fig.1. The two peaks along the  $x' = -x$  direction describe spatial coherences at the initial time (which we may denote as nonlocal). As

we have seen, the entanglement with the field-qubit environment causes a decoherence of  $\hat{\rho}(x, x'; t)$  in terms of a time decay of these two peaks. Because of the discreteness of the environment states density, the considerations brought in the previous section only indicate a propensity to a classical landing, as the figures of the previous section show.

As for the other two peaks located in the orthogonal direction, one could say that they describe the atomic populations, that is, the two possible atomic initial position [2]. Actually, when  $x'$  is near to but not coincident with  $x$ , the function  $\hat{\rho}(x, x'; 0)$  describes coherences (which we may denote as local). An intriguing question concerns the time evolution of these two peaks. First of all, the asymptotic form of the real part should give the genuine populations, however, for continuity reasons, the local coherences cannot abruptly vanish. The Fig. 8 reports  $Re[\hat{\rho}(x, x'; t)]$  along a direction parallel to  $(x' = -x)$ , thought one of the two maxima located in  $x_{0,i}$ . One may note how  $x_{0,1}$  asymptotically behaves as an accumulation point for the local coherences.

As far as the imaginary part is concerned, also in this case a decay similar to what happens for the nonlocal coherences cannot be granted. In fact, as seen in sec. 3, the mean value of the atomic momentum is connected to the  $Im[\hat{\rho}(x, x'; t)]$ . More precisely, since in our case  $Im[\hat{\rho}(x, x'; 0)] = 0$  (and  $\langle \hat{p} \rangle (0) = 0$ ), an increasing mean value of  $\langle \hat{p} \rangle$  requires a non vanishing imaginary decoherence factor, as one may see from Eq.s (38) and (36). We find, in fact, that the local imaginary coher-

ences are not subjected to an asymptotical decay, as Fig. 9 shows. Since  $\langle \hat{p} \rangle (0) = 0$ , the function  $Im[\hat{\rho}(x' = -x + 2x_{0,1}; t)]$  grows up from zero, and for  $t$  sufficiently large, its amplitude behaves similarly to the real case of Fig. 8, with an essential difference: at the accumulation point  $x_{0,1}$ ,  $Im[\hat{\rho}(x' = -x + 2x_{0,1}; t)]$  is zero, with an increasing slope which accounts for the atomic acceleration.

## 6 Conclusions

The optical Stern-Gerlach model is a useful tool for analyze disentanglement and decoherence processes that involve environments with a few degrees of freedom both for discrete and continuous variables. It consists essentially of a Jaynes-Cummings two level atom which entangles with its translational dynamics along the cavity axis. Under the environmental action of the Jaynes-Cummings qubit we analyze the decoherence process of the atomic translation, considered as system of interest. We find that the decoherence features may be encoded into a decoherence function  $D(x, x'; t)$ . In fact, for the more general one mode state (pure or mixed) of the cavity field, the atomic spatial density matrix may be factorized as  $\rho(x, x'; t) = \rho(x, x'; 0) D(x, x'; t)$ , where the decoherence factor  $D(x, x'; t)$  depends on the statistics and on the phase properties of the field. The field statistics affects  $D(x, x'; t)$  through the density of quantum paths followed in the interchange of energy and information between the subsystems, while the phase properties of the field (more precisely, the qubit-field phase relations) are related to the imaginary part of  $D(x, x'; t)$  and to the atomic kinematics.

We find useful to distinguish the local coherences  $\hat{\rho}(x' = -x + 2x_{0,i}; t)$  in the neighborhoods of the two population peaks,  $x \simeq x_{0,i} \simeq x'$  ( $i = 1, 2$ ), from the non local ones  $\hat{\rho}(x' = -x; t)$ , along the direction  $x' = -x$  (see Fig. 1). As expected,  $\hat{\rho}(x' = -x; t)$  asymptotically vanishes, with decay times depending on the environment states density, and consequently, on the field statistics (because of the discreteness of these states, the non local coherences are subjected to a partial revival at larger times). On the contrary, the local coherences cannot abruptly vanish, since their real part has to ensure the asymptotic survival of the populations. Surprisingly, also the imaginary local coherences do survive for increasing values of the atomic momentum, and the neighborhoods of the two population peaks asymptotically became a sort of accumulation points for the local coherences. In our opinion, these peculiarities of the local coherences deserve further analysis.

## References

1. H.D Zeh, *Found. Phys.* **1**, 69 (1970)
2. W.H. Zurek, *Phys. Today* **44**, 36 (1991)
3. W.H. Zurek, *Rev. Mod. Phys.* **75**, 715 (2003)
4. M. Schlosshauer, *Rev. Mod. Phys.* **76**, 1267 (2005)
5. E. Joos, H.D Zeh, C. Kiefer, D. Giulini, J. Kupsch, and I.-O. Stamatescu, *Decoherence and the Appearance of a Classical World in Quantum Theory*, Springer, New York, 2nd edition (2003)
6. M. Schlosshauer, *Decoherence and the Quantum-to-Classical Transition*, Springer, (2007)
7. N.P. Landsmann, *Stud. Hist. Phil. Mod. Phys.* **26**, 45 (1995)
8. M. Brune, E. Hagley, J. Dreyer, X. Maître, A. Maali, C. Wunderlich, J.M. Raimond, and S. Haroche *Phys. Rev. Lett.* **77**, 4887 (1996)
9. J.M. Raimond, M. Brune, and S. Haroche, *Rev. Mod. Phys.* **73**, 565 (2001)
10. P. Storey, M. Collett, and D. Walls, *Phys. Rev. Lett.* **68**, 472 (1992)
11. P. Storey, M. Collett, and D. Walls, *Phys. Rev. A* **47**, 405 (1993)
12. M. Scully, B-G. Englert, H. Walther, *Nature* **351**, 111 (1991)
13. P. Storey, S. Tan, M. Collett, and D. Walls, *Nature* **367**, 626 (1994)
14. S. Dürr, T. Nonn, and G. Rempe, *Nature* **395**, 33 (1998)
15. Q. Jie, B. Hu, and G. Dong, quant-ph/0601025
16. A. Vaglica, *Phys. Rev. A* **58**, 3856 (1998)
17. A. Vaglica and G. Vetri, *Phys. Rev. A* **75**, 062120 (2007)
18. L. You, *Phys. Rev. A* **64**, 012302 (2001)
19. S. Shresta and B. L. Hu, *Phys. Rev. A* **68**, 012110 (2003)
20. M. Tumminello, A. Vaglica, and G. Vetri, *Europhys. Lett.* **65**, 785 (2004)
21. L. Zheng, C. Li, Y. Li, and C.P. Sun, *Phys. Rev. A* **71**, 062101 (2005)
22. M. Tumminello, A. Vaglica, and G. Vetri, *Europhys. Lett.* **66**, 792 (2004)
23. M. Tumminello, A. Vaglica, and G. Vetri, *Eur.Phys. J. D* **36**, 235 (2005)
24. M. Chianello, M. Tumminello, A. Vaglica, and G. Vetri, *Phys. Rev. A* **69**, 053403 (2004)
25. See sec. III.B of Ref. [17]

26. L. Susskind and J. Glogower, *Physics (Long Island City, NY)* **1**, 49 (1964); P. Carruthers and M.M. Nieto, *Rev. Mod. Phys.* **40**, 411 (1968)
27. J.I. Cirac and L.L. Sánchez-Soto, *Phys. Rev. A* **42**, 2851 (1990)
28. I. Cusumano, A. Vaglica, and G. Vetri, *Phys. Rev. A* **66**, 043408 (2002)
29. N.B. Narozhny, J.J. Sanchez-Mondragon, and J.H. Eberly, *Phys. Rev. A* **23**, 236 (1981)
30. G. Rempe, H. Walther, and N. Klein, *Phys. Rev. Lett* **58**, 353 (1987)
31. P.L. Knight and P.M. Radmore, *Phys. Lett. A* **90**, 342 (1982)
32. C. Riti and G. Vetri, *Optics Commun.* **44**, 105 (1982)
33. S.M. Barnett, P. Filipowicz, J. Javanainen, P.L. Knight, and P. Meystre, in *Frontiers in Quantum Optics*, ed. by E.R. Pike and S. Sarkar (Bristol: Adam Hilger), 485 (1986)
34. O. Pessoa Jr., *Sinthese* **113**, 323 (1998)
35. K. Zaheer and M.S. Zubairy *Phys. Rev. A* **39**, 2000 (1989)